Density-functional theory of freezing of quantum liquids at zero temperature using exact liquid-state linear response

C. N. Likos*
Dipartimento di Fisica Teorica dell'Università di Trieste and Istituto Nazionale di Fisica della Materia, Strada Costiera 11, I-34014 Grignano, Trieste, Italy

Saverio Moroni†
International Centre for Theoretical Physics, Strada Costiera 11, I-34014 Trieste, Italy

Gaetano Senatore‡
Dipartimento di Fisica Teorica dell'Università di Trieste and Istituto Nazionale di Fisica della Materia, Strada Costiera 11, I-34014 Grignano, Trieste, Italy

(Received 27 August 1996)

We apply density-functional theory to study the freezing of superfluid ^{4}He, charged bosons, and charged fermions at zero temperature. We employ accurate quantum Monte Carlo data for the linear-response function in the uniform phase of these systems, a quantity that has different behavior for large values of the wave vector than previously assumed. We find that, as a result of this *exact* behavior, different approximations in the density-functional theory of freezing that involve linear response, all fail to correctly describe the crystallization in *three dimensions*, while yielding satisfactory predictions in *two dimensions*. This demonstrates the shortcomings of the currently popular density-functional approximate theories to describe $3d$ freezing in the quantum regime. We also investigate the consequences of the exact asymptotic behavior of response functions on the form of effective interactions and polarization potentials in the electron gas, at small distances. [S0163-1829(97)04310-5]

I. INTRODUCTION

The modern density-functional theory (DFT), which is employed in the theoretical investigations of freezing of both quantal and classical systems, is based on an exact correspondence between equilibrium one-particle densities and external potentials.[1,2] In particular, if we denote by $n(\mathbf{r})$ the one-particle density of the system (i.e., the statistical average of the one-particle density operator) the system can be characterized by an appropriate thermodynamic potential which attains its minimum value for the correct (equilibrium) profile $n_0(\mathbf{r})$. For the study of crystallization, the relevant thermodynamic potentials are the grand potential Ω and the intrinsic Helmholtz free energy F, the latter being a *unique functional* of the one-particle density.[1,2] If μ is the chemical potential of the system at some temperature T and $v_{\rm ext}(\mathbf{r})$ is an arbitrary external potential, then the quantity:

$$\widetilde{\Omega}[n,u]=F[n]-\int d\mathbf{r}n(\mathbf{r})u(\mathbf{r}), \tag{1.1}$$

where $u(\mathbf{r})=\mu-v_{\rm ext}(\mathbf{r})$, is a *minimum* for given $u(\mathbf{r})$ at the equilibrium density $n_0(\mathbf{r})$. The quantity $\Omega[u]=\widetilde{\Omega}[n_0,u]$ is then the grand potential of the system. Clearly, the equilibrium condition reads as

$$\frac{\delta F[n]}{\delta n(\mathbf{r})}\Big|_{n_0(\mathbf{r})}=u(\mathbf{r}). \tag{1.2}$$

For vanishing external potential and fixed particle number N, the intrinsic free energy $F[n]$ is a minimum at the equilibrium density, with respect to variations of the *shape* of the density profile. It is customary to separate $F[n]$ into a contribution from the noninteracting system under a suitable external potential that makes $n(\mathbf{r})$ the equilibrium density, $F_{\rm id}[n]$, and an excess part $F_{\rm ex}[n]$, i.e., $F[n]=F_{\rm id}[n]+F_{\rm ex}[n]$. The determination of F_{id} is not complicated, for both classical and quantum systems: in the former case, $F_{\rm id}$ is known explicitly as a functional of the density.[3] In the latter case, the statistics appears explicitly in the construction of $F_{\rm id}$, and for given external potential one can construct both the equilibrium density and $F_{\rm id}$ in a straightforward manner. Therefore, the art of density-functional theory amounts to the invention of approximate functionals for the excess part. In the classical regime, there has been extensive work in this direction during the last 15 years.[4] Relatively less has been done in the quantum regime, with which we are concerned in this work.

The development of quantum DFT of freezing has followed two alternative routes: In one case,[5] suitable for finite temperatures, a mapping of the quantum particles into classical polymer rings is invoked; in the other, which is better suited for zero temperature, the Hohenberg-Kohn-Sham formalism[1,6] is used, and the problem is reduced to a self-consistent band-structure calculation.[7–9] Here we follow the second approach, since we are interested in $T=0$ freezing. In this case, $F[n]$ is simply the intrinsic ground-state energy $E[n]$. The ideal part $F_{\rm id}[n]$ reduces to the kinetic energy of noninteracting particles $T_0[n]$, and the remainder $F_{\rm ex}[n]$ is the excess energy $E_{\rm ex}[n]$. A brief summary of this formalism will be presented below.

Within certain classes of approximate functionals, an essential ingredient for the practical implementation of this approach is the linear-response function $\chi(r;n)$ of the fluid, or its Fourier transform $\tilde{\chi}(q;n)$ where q is the wave-vector magnitude and n is the average density. In particular, what is important is the ''quantum'' direct correlation function (dcf), i.e., *the difference* between the inverse linear-response functions of the interacting and noninteracting systems, $\tilde{K}(q,n)=\tilde{\chi}^{-1}(q;n)-\tilde{\chi}_0^{-1}(q;n)$. In previous applications[7–10] it was assumed that this difference is asymptotically vanishing (maybe in an oscillatory manner) for large values of the wave vector. However, recent exact results,[11,12] and associated quantum Monte Carlo (QMC) calculations[13–15] show that this is not the case: instead, the aforementioned difference approaches a *positive constant* as $q\to\infty$. In this paper, we revisit the DFT of freezing, using the correct liquid-state input. We examine the performance of the perturbative second-order theory[16] (SOT) and the nonperturbative modified weighted density approximation (MWDA).[17] For a variety of systems, and irrespective of the range of the interaction and the statistics (superfluid ^{4}He, charged bosons and fermions), we find that this *exact* large-q behavior has drastic consequences in three spatial dimensions: the crystal is predicted to be the stable phase for any density. The SOT-functional is affected by this behavior most dramatically: it becomes unbounded from below as the density becomes more localized around the lattice sites and thus it has a minus-infinity minimum at a perfectly localized density. The MWDA, on the other hand, does not suffer from this extreme pathology: the MWDA functional is bounded from below, but the (finite) minimum of the energy always occurs for a modulated (crystal) phase. In two dimensions, the effect is much less drastic, in the sense that for densities relevant to crystallization the SOT functional continues to be bounded from below, yielding satisfactory predictions for the freezing of the electron gas.

The rest of this paper is organized as follows: in Sec. II we present a summary of the DFT formalism; in Sec. III we survey the liquid-state input and discuss its implications on the behavior of the ''quantum'' direct correlation functions, as well as on effective interactions—in the electrons gas; in Sec. IV we apply the SOT and in Sec. V the MWDA to the problem of freezing of different quantum liquids. Finally, in Sec. VI we summarize and conclude.

II. QUANTUM DENSITY-FUNCTIONAL THEORY OF FREEZING

The quantum DFT formalism employed in this work has been presented in detail in Refs. 7 and 9. Here we give only an outline and refer the reader to the above papers for details. Writing $E[n]=T_0[n]+E_{\rm ex}[n]$ and using Eqs. (1.1) and (1.2) we see that a *necessary* condition for equilibrium is

$$\left[\frac{\delta T_0[n]}{\delta n(\mathbf{r})}+\frac{\delta E_{\rm ex}[n]}{\delta n(\mathbf{r})}\right]_{n_0(\mathbf{r})}=\mu-v_{\rm ext}(\mathbf{r}), \tag{2.1}$$

for the case of interacting particles. This is formally equivalent to the condition of equilibrium for *noninteracting* particles (for which $E[n]=T_0[n]$) under the influence of an effective external potential

$$v_{\rm eff}(\mathbf{r})=\frac{\delta E_{\rm ex}[n]}{\delta n(\mathbf{r})}+v_{\rm ext}(\mathbf{r}). \tag{2.2}$$

Note that the effective potential is itself a functional of the one-particle density, through the dependence of $E_{\rm ex}[n]$ on $n(\mathbf{r})$. Therefore, one is faced with a *self-consistency* calculation which in practice proceeds as follows: an initial guess is made for the density profile, which yields an initial form for the effective potential. Then the one-particle Schrödinger equations (Kohn-Sham equations)

$$\left[-\frac{\hbar^2}{2m}\nabla^2+v_{\rm eff}(\mathbf{r})\right]\psi_i(\mathbf{r})=\varepsilon_i\psi(\mathbf{r}) \tag{2.3}$$

are solved, yielding the eigenfunctions $\psi_i(\mathbf{r})$ and the associated energy eigenvalues ε_i. From the former, a new one-particle density is constructed through

$$n(\mathbf{r})=\sum_i n_i|\psi_i(\mathbf{r})|^2, \tag{2.4}$$

where n_i are the occupation numbers suitable for the given statistics (Bose or Fermi). The new density serves for the construction of the new effective potential, and the cycle is continued until a self-consistent solution has been found. Once the self-consistent orbitals $\psi_i(\mathbf{r})$ and the associated eigenvalues ε_i and density $n_0(\mathbf{r})$ are known, the ideal kinetic energy T_0 is given by

$$\begin{aligned}T_0&=\sum_i n_i\int d\mathbf{r}\psi_i^*(\mathbf{r})\left(-\frac{\hbar^2}{2m}\nabla^2\right)\psi_i(\mathbf{r})\\&=\sum_i n_i\varepsilon_i-\int d\mathbf{r}n_0(\mathbf{r})v_{\rm eff}(\mathbf{r}).\end{aligned} \tag{2.5}$$

The formulation presented above is *exact*, provided v representability holds.[18] Approximations enter through the excess energy functional $E_{\rm ex}[n]$ which is not known exactly. In the following subsections we present two common schemes which both rely on the knowledge of the second functional derivative of this functional with respect to the density at the uniform limit. This quantity is in turn directly related to the density-density linear-response function.

A. Second-order theory

One usual approximation is the so-called second order theory (SOT) or quadratic approximation. Here, one expands functionally the unknown functional about a uniform fluid of density n_l, keeping terms up to second-order only. Explicitly,

$$\begin{aligned}E_{\rm ex}[n]=E_{\rm ex}(n_l)&+\int d\mathbf{r}\left.\frac{\delta E_{\rm ex}[n]}{\delta n(\mathbf{r})}\right|_{n_l}\delta n(\mathbf{r})\\&+\frac{1}{2}\int\int d\mathbf{r}d\mathbf{r}'\left.\frac{\delta^2 E_{\rm ex}[n]}{\delta n(\mathbf{r})\,\delta n(\mathbf{r}')}\right|_{n_l}\delta n(\mathbf{r})\,\delta n(\mathbf{r}'),\end{aligned} \tag{2.6}$$

with $\delta n(\mathbf{r})=n(\mathbf{r})-n_l$ and $E_{\rm ex}(n_l)$ the excess intrinsic energy of the uniform liquid, a *function* of n_l. Due to the translational and rotational invariance of the liquid, the first

functional derivative in the right-hand side (rhs) of Eq. (2.6) is just a position-independent constant, equal to the excess chemical potential of the homogeneous liquid. The second functional derivative is a function of $|\mathbf{r}-\mathbf{r}'|$ only; both depend on n_l, of course. We define, from now on,

$$\left.\frac{\delta^2 E_{\rm ex}[n]}{\delta n(\mathbf{r})\,\delta n(\mathbf{r}')}\right|_{n_l} \equiv -K(|\mathbf{r}-\mathbf{r}'|;n_l). \tag{2.7}$$

The function $K(r;n)$ is the excess part of the linear static inverse response function of the homogeneous liquid, and can also be expressed as[7]

$$K(r;n)=\chi^{-1}(r;n)-\chi_0^{-1}(r;n), \tag{2.8}$$

where $\chi^{-1}(r;n)$ and $\chi_0^{-1}(r;n)$ are the functional inverses[19] of the density-density static linear-response functions of the interacting and noninteracting liquid, respectively.

Such an approximation is not *a priori* guaranteed to have any validity, since there is no ''small parameter'' guiding the expansion. Its widespread use is due on the one hand to practical limitations, as third- and higher-order functional derivatives of $E_{\rm ex}[n]$ are poorly known even in the uniform phase, and on the other hand, in the relative success that it has had, at least in the classical regime, in predicting the freezing parameters of simple liquids.[4] The function $K(r;n_l)$ is *formally* the quantum analog of the classical Ornstein-Zernicke direct correlation function (dcf).[20]

We set $v_{\rm ext}(\mathbf{r})=0$ from now on. In the quadratic approximation for the excess part of the energy functional, the effective potential which enters in the Kohn-Sham calculation is periodic with Fourier components

$$v_{\rm eff}(\mathbf{Q})=\delta n_{\mathbf{Q}}[-\tilde{\chi}^{-1}(Q;n_l)+\tilde{\chi}_0^{-1}(Q;n_l)], \tag{2.9}$$

where $\mathbf{Q}$ is a reciprocal-lattice vector (RLV) of the given lattice and $\delta n_{\mathbf{Q}}$ is the Fourier component of the periodic function $\delta n(\mathbf{r})\equiv n(\mathbf{r})-n_l$, and $\tilde{\chi}^{-1}(q;n_l)$ is the Fourier transform of the function $\chi^{-1}(r;n_l)$.

For systems of neutral particles, the choice of the density n_l of the reference liquid is arbitrary, although the usual choice is to consider a liquid at the same chemical potential as the solid. Moreover, for a Bose system at $T=0$ the kinetic energy of independent particles vanishes in the uniform limit. Thus, the difference between the grand potential[21] of the solid and the liquid is[10]

$$\begin{aligned}\Delta\Omega[n]&=T_0[n]-\frac{1}{2}\int\int d\mathbf{r}d\mathbf{r}'K(|\mathbf{r}-\mathbf{r}'|;n_l)\,\delta n(\mathbf{r})\,\delta n(\mathbf{r}')\\&=T_0[n]-\frac{V}{2}\tilde{K}(0;n_l)(n_s-n_l)^2\\&\quad-\frac{V}{2}\sum_{\mathbf{Q}\neq\mathbf{0}}|n_{\mathbf{Q}}|^2\tilde{K}(Q;n_l).\end{aligned} \tag{2.10}$$

In Eq. (2.10), V is the volume of the system, n_s is the average density of the solid, $\tilde{K}(q;n)$ denotes the Fourier transform of $K(r;n)$ at wave vector q, and $n_{\mathbf{Q}}$ is the Fourier component of the periodic density at RLV $\mathbf{Q}$. In practice, one changes μ (or, equivalently, n_l) and minimizes $\Delta\Omega[n]$ with respect to $n(\mathbf{r})$. Freezing occurs when $\min\{\Delta\Omega[n]\}$ vanishes. For $\min\{\Delta\Omega[n]\}>0$ (<0) the liquid (solid) is stable.

For systems composed of particles carrying a charge e and interacting via the Coulomb potential $v_c(r)=e^2/r$, the presence of a uniform, rigid, neutralizing background of opposite charge guarantees the stability of the system. The presence of the background imposes the constraint that the freezing transition now takes place *at constant density* (isochoric freezing). The relevant thermodynamic potential is now the total energy $E[n]$; the phase with the lowest $E[n]$ is the thermodynamically stable one. It is customary for such systems to separate the excess energy into a Hartree contribution and an ''exchange-correlation'' contribution, i.e., to write

$$E_{\rm ex}[n]=\frac{e^2}{2}\int\int d\mathbf{r}d\mathbf{r}'\frac{\delta n(\mathbf{r})\,\delta n(\mathbf{r}')}{|\mathbf{r}-\mathbf{r}'|}+E_{\rm xc}[n], \tag{2.11}$$

where $\delta n(\mathbf{r})=n(\mathbf{r})-\overline{n}$ and $\overline{n}$ is the average density. If we now define

$$\left.\frac{\delta^2 E_{\rm xc}[n]}{\delta n(\mathbf{r})\,\delta n(\mathbf{r}')}\right|_{n_l} \equiv -K_{\rm xc}(|\mathbf{r}-\mathbf{r}'|;n_l), \tag{2.12}$$

then Eqs. (2.7) and (2.11) imply

$$K(|\mathbf{r}-\mathbf{r}'|;n_l)=-v_c(|\mathbf{r}-\mathbf{r}'|)+K_{\rm xc}(|\mathbf{r}-\mathbf{r}'|;n_l). \tag{2.13}$$

In Fourier space, one writes the Fourier transform $\tilde{K}_{\rm xc}(q;n)$ of $K_{\rm xc}(r;n)$ as $\tilde{K}_{\rm xc}(q;n)=v_c(q)G(q;n)$, where $v_c(q)$ is the Fourier transform of the Coulomb potential $[v_c(q)=4\pi e^2/q^2$ in three dimensions and $2\pi e^2/q$ in two dimensions] and $G(q;n)$ is the so-called *local-field factor*.[22] Finally we have

$$-\tilde{K}(q;n)=v_c(q)[1-G(q;n)]. \tag{2.14}$$

Due to the long-range nature of the Coulomb potential, the functional expansion of the energy of the inhomogeneous phase can now be performed only about a liquid whose density n_l is *equal* to the average density $\overline{n}\equiv n_s$ of the solid. Using Eqs. (2.6), (2.7), (2.13), and (2.14) we obtain the difference between the energy[21] of the solid and the liquid phases as

$$\begin{aligned}\Delta E[n]&=T_0[n]-\frac{d}{d+2}N\epsilon_F\\&\quad+\frac{V}{2}\sum_{\mathbf{Q}\neq\mathbf{0}}|n_{\mathbf{Q}}|^2 v_c(Q)[1-G(Q;n_s)].\end{aligned} \tag{2.15}$$

Equation (2.15) above is valid for fermions in d dimensions with ϵ_F being the Fermi energy of noninteracting particles in the liquid phase. For bosons, this equation remains valid with the omission of the second term in the rhs.

As mentioned above, the lack of a small parameter in the functional expansion of the excess energy (at least as far as the freezing problem is concerned) has cast some doubt on the validity of the quadratic theory. This observation has led to the development of a class of nonperturbative approximations, which approximate the excess energy of the solid by that of a liquid. The density of the latter is a weighted average of the true density of the solid. Of particular interest, due

to its computational simplicity and its success in describing bulk freezing for certain model systems in the classical regime, is the modified weighted density approximation (MWDA) of Denton and Ashcroft,[17] presented in the following subsection.

B. Modified weighted density approximation

The MWDA amounts to the approximation of the excess energy of the modulated system by that of a uniform system at a weighted density[17,9] with the latter being evaluated as a weighted average over the real density of the crystal in a self-consistent way. In other words, one writes

$$E_{\rm ex}[n] \approx E_{\rm ex}^{\rm MWDA}[n] = N\epsilon(\hat{n}), \tag{2.16}$$

where $\epsilon(n)$ is the excess energy per particle of a uniform liquid of density n. The effective density $\hat{n}$ is evaluated as a weighted average over the spatially-varying density $n(\mathbf{r})$ of the crystal and is defined by

$$\hat{n} = \frac{1}{N}\int\int d\mathbf{r}d\mathbf{r}' n(\mathbf{r})n(\mathbf{r}')w(\mathbf{r}-\mathbf{r}';\hat{n}), \tag{2.17}$$

where the weight function $w(\mathbf{r}-\mathbf{r}';\hat{n})$, which depends on the weighted density itself is determined by requiring that the MWDA functional is exact to second-order in a functional expansion around a uniform liquid. The derivation of the expression for the weight function has been presented in detail elsewhere[9,17] and so here we show only the final results which read as

$$w(r;\hat{n}) = -\frac{1}{2\epsilon'(\hat{n})}\left(K(r;\hat{n}) + \frac{\hat{n}}{V}\epsilon''(\hat{n}) \right) \tag{2.18}$$

and

$$\hat{n} = n_s + \frac{1}{n_s}\sum_{\mathbf{Q}\neq\mathbf{0}} |n_{\mathbf{Q}}|^2 \frac{[-\tilde{K}(Q;\hat{n})]}{2\epsilon'(\hat{n})}. \tag{2.19}$$

The effective potential for the MWDA is readily calculated as[9]

$$v_{\rm eff}(\mathbf{r}) = \epsilon(\hat{n}) + \epsilon'(\hat{n})\frac{\delta\hat{n}}{\delta n(\mathbf{r})}, \tag{2.20}$$

and the corresponding expression in Fourier space, which is necessary for the solution of the MWDA-Kohn-Sham equations can be found in Ref. 9. The MWDA excess energy functional is exact to second order in a functional expansion about a reference liquid, but also includes contributions from all higher orders. In this sense, the MWDA is a nonperturbative approximate scheme for the calculation of the excess part of the energy.

C. The Gaussian ansatz

The self-consistent solution of the Kohn-Sham equations is sometimes avoided by taking advantage of the fact that, in the solid phase, the particles are well localized around the lattice sites. This leads to the introduction of the following Gaussian ansatz. One constructs normalized Bloch orbitals $\psi_{\mathbf{k}}(\mathbf{r})$ from a single Gaussian per site, $\phi(r) = (2\alpha/\pi)^{d/4}e^{-\alpha r^2}$, according to[23]

$$\psi_{\mathbf{k}}(\mathbf{r}) = \frac{1}{\sqrt{NP_0(\mathbf{k})}}\left(\frac{2\alpha}{\pi}\right)^{d/4}\sum_{\mathbf{R}} e^{i\mathbf{k}\cdot\mathbf{R}}e^{-\alpha(\mathbf{r}-\mathbf{R})^2}, \tag{2.21}$$

where $\{\mathbf{R}\}$ is the set of Bravais lattice vectors and

$$P_m(\mathbf{k}) = \sum_{\mathbf{R}} R^m e^{i\mathbf{k}\cdot\mathbf{R}-\alpha R^2/2}. \tag{2.22}$$

After some algebra, we arrive at the following explicit expressions for the noninteracting kinetic energy T_0 and the Fourier component of the density $n_{\mathbf{Q}}$:

$$T_0[n] = N\frac{\hbar^2}{2m}[d\alpha - \alpha^2\mu_2(\alpha)] \tag{2.23}$$

and

$$n_{\mathbf{Q}} = n_s e^{-Q^2/8\alpha}\mu_{\mathbf{Q}}, \tag{2.24}$$

where

$$\mu_2 = \frac{\sigma}{N}\sum_{\mathbf{k}}\frac{P_2(\mathbf{k})}{P_0(\mathbf{k})}, \quad \mu_{\mathbf{Q}} = \frac{\sigma}{N}\sum_{\mathbf{k}}\frac{P_0(\mathbf{k}-\mathbf{Q}/2)}{P_0(\mathbf{k})}. \tag{2.25}$$

Note that $T_0[n]$ remains positive definite for all values of α, as $\alpha^2\mu_2(\alpha)\to 0$ for strong localization (α large). Equations (2.23)–(2.25) above, are valid for fermions; σ denotes the number of particles in each occupied orbital: $\sigma=1$ for spin-polarized and $\sigma=2$ for unpolarized particles. The $\mathbf{k}$ sums extend over the occupied orbitals only. For bosons, we have to put all the particles in the same orbital, $\mathbf{k}=0$. In this case Eqs. (2.23) and (2.24) remain valid with the identification:

$$\mu_2 = \frac{P_2(0)}{P_0(0)}, \quad \mu_{\mathbf{Q}} = \frac{P_0(\mathbf{Q}/2)}{P_0(0)}. \tag{2.26}$$

Substituting the appropriate expression for T_0 and $n_{\mathbf{Q}}$ into Eqs. (2.10) or (2.15) above, one directly obtains the difference of the appropriate thermodynamic potential between the solid and the liquid, within the SOT. In the MWDA, the additional self-consistent solution of Eq. (2.19) is required to get the excess energy of Eq. (2.16). In both cases one ends up with differences of thermodynamic potentials as a function of α, n_s, and n_l. One then varies α (and n_s for neutral particles) until a minimum is found. By repeating the procedure for different values of n_l one can determine the phase diagram of the system at hand.

We are going to present results obtained mainly through the use of the Gaussian ansatz, rather than the full self-consistent calculation. The reason is that, if a minimum exists when the Gaussian ansatz is employed, then the full calculation can only yield a lower minimum since the class of Gaussian densities is only a subclass of all the possible profiles. Since our calculations yield *too low minima*, the self-consistent calculation is for most purposes redundant. Moreover, the Gaussian ansatz allows for analytical estimates of the magnitudes of the ideal and excess terms in Eq. (2.10) or (2.15).

The excess liquid-state linear static inverse-response function $K(r;n)$ plays, evidently, a central role in the implementation of the approximate schemes presented above. In the following section we discuss the form and asymptotic behavior of this function.

III. LIQUID-STATE INPUT, QUANTUM DIRECT CORRELATION FUNCTION, AND EFFECTIVE INTERACTIONS

For classical liquids, the Fourier transform of the dcf is related to the experimentally measured structure factor $S(q)$ by a simple algebraic relation,[20] by virtue of the fluctuation-dissipation theorem. For quantum systems, on the other hand, the theorem relates dynamical quantities, and the relation between static quantities is not simple any more.[7] As a result, various approximations for the static linear-response function $\tilde{\chi}(q)$ have been developed.

Superfluid ^{4}He is a test case. This is a fluid of neutral particles whose interactions can be accurately described by the so-called Aziz potential.[24,25] In the absence of accurate data for $\tilde{\chi}(q)$, one often resorts to the Feynman approximation to obtain a relation between $\tilde{\chi}(q)$ and $S(q)$,[10] which reads as

$$\tilde{\chi}_F(q;n_l)=\tilde{\chi}_0(q;n_l)S^2(q), \tag{3.1}$$

where $\tilde{\chi}_0(q;n_l)=-4mn_l/\hbar^2q^2$ is the static susceptibility of the ideal boson gas. The ensuing approximate dcf

$$\tilde{K}_F(q;n_l)=\frac{\hbar^2q^2}{4mn_l}\left(1-\frac{1}{S^2(q)}\right) \tag{3.2}$$

has been employed in density-functional theories of freezing of ^{4}He (Refs. 10,26) or Bose hard spheres[8] albeit with an appropriate ''rescaling'' which was employed in an empirical way. This rescaling has been avoided in a recent density-functional study of quantum hard-sphere freezing.[27] However, accurate data for $\tilde{\chi}(q)$ have now been obtained from diffusion Monte Carlo calculations.[13] In Fig. 1 we show plots of this *accurate* direct correlation function for three different densities of the liquid. A comparison with the Feynman approximation[10] shows immediately that whereas the latter has an oscillatory behavior about zero, the exact dcf is negative for almost all values of $q>2$ Å^{-1}. An additional important difference concerns the large-q behavior of the dcf. Although the Monte Carlo data are limited to values $q<4-6$ Å^{-1}, exact theoretical calculations[12] imply that the $q\to\infty$-limit of $-\tilde{K}(q,n_l)$ is a negative number (see below), and not zero as in the Feynman approximation[28] Eq. (3.2). In particular, the response function $\tilde{\chi}(q;n_l)$ is given for large q by[12]

$$\tilde{\chi}(q;n_l)=-\frac{4mn_l}{\hbar^2q^2}\left[1+\frac{8m}{3\hbar^2q^2}\langle KE\rangle+O(q^{-4})\right], \tag{3.3}$$

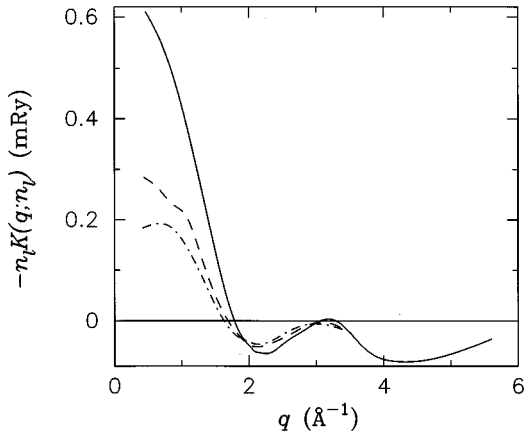

FIG. 1. The function $-n_l\tilde{K}(q;n_l)$ (in mRy) of superfluid ^{4}He as obtained from simulations (Ref. 13), for three different fluid densities. Solid line: $n_l=0.026\,22$ Å^{-3}; dashed line: $n_l=0.021\,86$ Å^{-3}; dash-dotted line: $n_l=0.019\,64$ Å^{-3}. The very accurate kinetic energies of Ref. 41 yield $-n_l\tilde{K}(\infty;n_l)(\text{mRy})=-0.0815$, -0.0593, -0.0493, in order of decreasing density.

From Eqs. (2.8), (3.3) and using the result $\tilde{\chi}_0(q;n_l)=-4mn_l/\hbar^2q^2$ for the static susceptibility of the ideal boson gas, we obtain

$$-n_l\tilde{K}(\infty;n_l)=-\tfrac{2}{3}\langle KE\rangle, \tag{3.4}$$

where $\langle KE\rangle$ is the expectation value of the kinetic energy in the liquid phase. These features of the exact dcf have important consequences on the performance of DFT's of freezing, as will be shown below.

Charged fermions or bosons are another example of quantum liquids. The former is just the usual system of electrons in a uniform background (jellium) and the latter is a model system of spinless particles of electronic charge e and mass m in a background, but obeying Bose statistics. A natural length scale for these systems is the so-called Wigner-Seitz radius r_0 defined as the radius of a sphere which contains, on average, one particle, i.e., for a system of density n in d dimensions we have

$$n=\frac{3}{4\pi r_0^3}\quad(d=3),\qquad n=\frac{1}{\pi r_0^2}\quad(d=2). \tag{3.5}$$

A convenient dimensionless measure of the density is $r_s\equiv r_0/a_0$, where a_0 is the Bohr radius. A widely used scheme to relate the local-field factor $G(q)$ with the structure factor has been introduced by Singwi, Tosi, Land, and Sjölander[29] (STLS). This has been employed in DFT's of freezing of jellium in a number of cases.[7,9] An important feature of the STLS scheme is that in the limit of large-q the local-field factor $G(q)$ approaches unity and this implies that $-\tilde{K}(q;n_l)$ approaches zero in that limit [see Eq. (2.14)]. In this respect, the STLS scheme for systems of charged particles has the same features as the Feynman approximation. However, it has been shown *exactly* that in the large-q limit, $G(q)$ goes like q^2 in three dimensions;[11,12] moreover it can

easily be shown that it scales like q in two dimensions.[30] In particular, for charged bosons at $d=3$ it is known that[15] for large q,

$$G(q;n_l)=\frac{2\langle KE\rangle q^2}{3m\omega_{\rm pl}^2}+\frac{2}{3}[1-g(0)]+\frac{16\langle (KE)^2\rangle}{5\hbar^2\omega_{\rm pl}^2}-\frac{16\langle KE\rangle^2}{9\hbar^2\omega_{\rm pl}^2}+O(q^{-2}), \tag{3.6}$$

where $\omega_{\rm pl}=\sqrt{4\pi n_l e^2/m}$ is the plasma frequency and $g(0)$ is the value of the pair distribution function of the liquid $g(r)$ at zero separation. From Eqs. (2.14) and (3.6) we find once more

$$-n_l\widetilde{K}(\infty;n_l)=-\frac{2}{3}\langle KE\rangle, \tag{3.7}$$

as in Eq. (3.4) above.

For fermions in three dimensions, the large q local-field factor reads as[11,31]

$$G(q;n_l)=\frac{2(\langle KE\rangle-\langle KE\rangle_0)q^2}{3m\omega_{\rm pl}^2}+\frac{2}{3}[1-g(0)]+\frac{16(\langle (KE)^2\rangle-\langle (KE)^2\rangle_0)}{5\hbar^2\omega_{pl}^2}-\frac{16(\langle KE\rangle^2-\langle KE\rangle_0^2)}{9\hbar^2\omega_{\rm pl}^2}+O(q^{-2}), \tag{3.8}$$

where $\langle\cdots\rangle_0$ denotes a noninteracting average, and the coefficient of the q^2 term—the difference in the kinetic energy per particle between the interacting and the noninteracting system—is a positive quantity.[11,31] Note that the differences between Eq. (3.8) and Eq. (3.6) arise from the different momentum distributions of the noninteracting Fermi and Bose systems. Using Eqs. (2.14), (3.8) we finally obtain

$$-n_l\widetilde{K}(\infty;n_l)=-\tfrac{2}{3}(\langle KE\rangle-\langle KE\rangle_0). \tag{3.9}$$

In Fig. 2 we show the direct correlation function of charged bosons for a number of different densities as obtained from quantum Monte Carlo simulations.[15] In Fig. 3 we show the same function for fully polarized charged fermions at $r_s=100$, which has also been obtained from QMC.[32] In both cases, it is clearly seen that at large values of q the function $-\widetilde{K}(q;n_l)$ tends to a negative constant. In the system of point charged particles, by virtue of the virial theorem, this constant may be expressed most simply as

$$-n_l\widetilde{K}(\infty;n_l)=\frac{2}{3}\frac{d(r_sE)}{dr_s}, \tag{3.10}$$

with $E=\epsilon_c(r_s)$ the correlation energy per particle, for fermions, and $E=\epsilon(r_s)$ the energy per particle, for bosons.

In two dimensions, the situation is quite similar. For fermions, using the asymptotic behavior of the static linear-response function,[33] it has been shown[30] that the local-field factor scales linearly with q, as $q\to\infty$, namely,

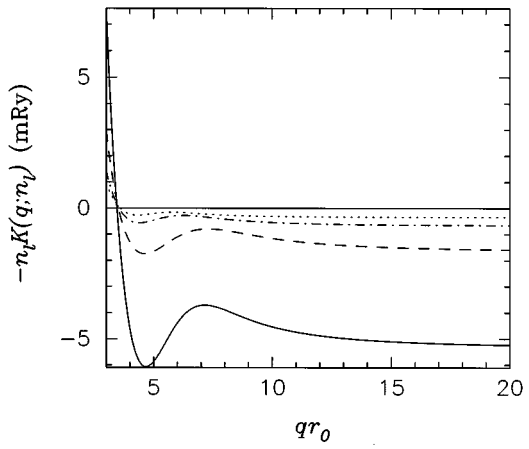

FIG. 2. The function $-n_l\widetilde{K}(q;n_l)$ (in mRy) of charged bosons as obtained from simulations (Ref. 15): solid line: $r_s=20$; dashed line: $r_s=50$; dash-dotted line: $r_s=100$; dotted line: $r_s=160$. The virtually exact kinetic energies of Ref. 15 yield $-n_l\widetilde{K}(\infty;n_l)$ (mRy) $=-5.27,-1.67,-0.665,-0.345$, in order of increasing r_s.

$$G(q;n_l)=\frac{(\langle KE\rangle-\langle KE\rangle_0)}{2\pi e^2 n_l}q+1-g(0)+O(q^{-1}). \tag{3.11}$$

From Eqs. (2.14) and (3.11) we obtain

$$-n_l\widetilde{K}(\infty;n_l)=-(\langle KE\rangle-\langle KE\rangle_0). \tag{3.12}$$

In Fig. 4 we show the direct correlation function of fully polarized electrons in two dimensions, near freezing, i.e., at $r_s=40$, as obtained from quantum Monte Carlo simulations.[32] Again, the saturation of $\widetilde{K}(q,n_l)$ to a constant—which may be conveniently expressed as

$$-n_l\widetilde{K}(\infty;n_l)=-(\langle KE\rangle-\langle KE\rangle_0)=\frac{d(r_s\epsilon_c)}{dr_s}, \tag{3.13}$$

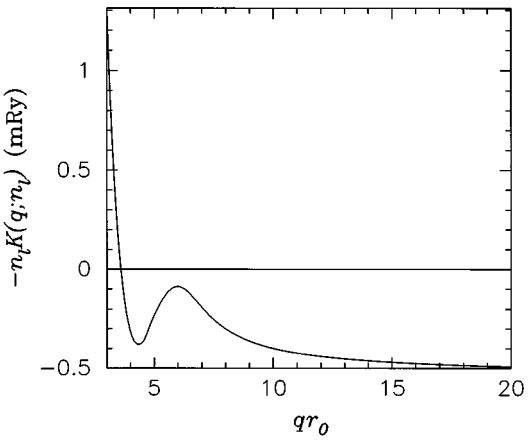

FIG. 3. The function $-n_l\widetilde{K}(q;n_l)$ (in mRy) of spin-polarized charged fermions, as obtained from simulations (Ref. 32), at $r_s=100$. The very accurate kinetic energy obtained from the fit of Ref. 39 yields $-n_l\widetilde{K}(\infty;n_l)=-0.527$ (mRy).

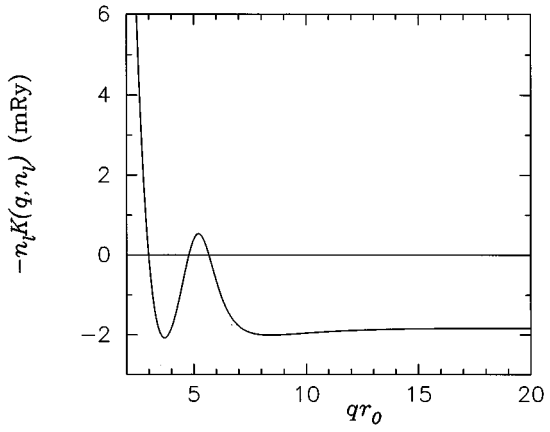

FIG. 4. The function $-n_l\widetilde{K}(q;n_l)$ (in mRy) of spin-polarized charged fermions in $2d$, as obtained from simulations (Ref. 32) at $r_s=40$. The very accurate kinetic energy of Ref. 43 yields $-n_l\widetilde{K}(\infty;n_l)=-1.88$ (mRy).

with $\epsilon_c(r_s)$ the correlation energy per particle—is evident. We note that the large-q behavior of $-n_l\widetilde{K}(q,n_l)$ for all the systems considered above is given by

$$-n_l\widetilde{K}(q,n_l)=-\frac{2}{d}(\langle KE\rangle-\langle KE\rangle_0)+O(q^{-d+1})+O(q^{-2}), \tag{3.14}$$

and evidently for the noninteracting Bose systems $\langle KE\rangle_0=0$. In fact one may easily show[34,12,27] that Eq. (3.14) above is valid for any quantum liquid interacting with pair potentials, both in three and two dimensions, provided the second term on the rhs is only retained for Coulombic systems ($1/r$ interaction) in two dimensions.

The short-wavelength behavior of $-\widetilde{K}(q;n_l)$ described above, implies that in real space the function $-K(r;n_l)$ has a δ-function contribution at the origin with negative weight, as is clear from Eq. (3.14). We shall therefore define a regular dcf $\widetilde{K}_R(q;n_l)$, decaying to zero as $q\to\infty$, by setting

$$\widetilde{K}(q;n_l)=\widetilde{K}_R(q;n_l)+\frac{2}{n_l d}(\langle KE\rangle-\langle KE\rangle_0). \tag{3.15}$$

This implies in real space

$$\begin{aligned}K(r;n_l)&=K_R(r;n_l)+U_0(n_l)\,\delta(\mathbf{r})n_l^{-1}\\&\equiv K_R(r;n_l)+K_S(r;n_l),\end{aligned} \tag{3.16}$$

with the strength of the singular part $K_S(r;n_l)$ given by

$$U_0(n_l)=\frac{2}{d}(\langle KE\rangle-\langle KE\rangle_0)>0. \tag{3.17}$$

Before investigating the consequences of this unexpected behavior of $-K(r;n_l)$ on the density functional theories of freezing, we shall pause here to briefly discuss its implications on effective interparticle interactions in the liquid phase. As an example we shall consider spin-unpolarized electrons in three dimensions.

Within the dielectric formalism, the number and spin linear-response functions of the normal electron fluid may be cast in a mean-field, random-phase-approximation-like form, by defining appropriate polarization potentials.[35] In the static limit to which we shall restrict here, the number and spin-response functions read, respectively,

$$\widetilde{\chi}(q)=\frac{\widetilde{\chi}_0(q)}{1-V^s(q)\widetilde{\chi}_0(q)} \tag{3.18}$$

and

$$\widetilde{\chi}_s(q)=-\mu_B^2\frac{\widetilde{\chi}_0(q)}{1-V^a(q)\widetilde{\chi}_0(q)}, \tag{3.19}$$

with μ_B the Bohr magneton and $V^s(q)$ and $V^a(q)$ the symmetric and asymmetric polarization potentials, respectively.[35,33] From Eqs. (2.8) and (2.14) it follows that

$$V^s(q)=-\widetilde{K}(q,n_l)=v_c(q)[1-G^s(q,n_l)], \tag{3.20}$$

with $G^s(q,n_l)\equiv G(q,n_l)$. In a similar fashion one can set[33]

$$V^a(q)=-v_c(q)G^a(q,n_l), \tag{3.21}$$

which defines the asymmetric local-field factor $G^a(q,n_l)$, whose behavior for large q is easily obtained from the known asymptotic expansions of $\widetilde{\chi}_s(q)$ (Ref. 33) as

$$G^a(q,n_l)=G^s(q,n_l)-1+2g(0)+O(q^{-2}). \tag{3.22}$$

Interparticle polarization potentials for pairs of electrons with parallel or antiparallel spin projections are readily obtained from their symmetric and asymmetric counterparts $V^s(q)$ and $V^a(q)$ via[35]

$$V^{\rm pol}_{\sigma\sigma'}(q)=V^s(q)\pm V^a(q)=v_c[1-G^s(q,n_l)\mp G^a(q,n_l)], \tag{3.23}$$

where the upper sign corresponds to $\sigma\sigma'=\uparrow\uparrow$ and the lower to $\sigma\sigma'=\uparrow\downarrow$. For large q, from Eqs. (3.8) and (3.22) one obtains

$$V^{\rm pol}_{\uparrow\uparrow}(q)=-\frac{4}{3n_l}(\langle KE\rangle-\langle KE\rangle_0)+O(q^{-2}) \tag{3.24}$$

and

$$V^{\rm pol}_{\uparrow\downarrow}(q)=2g(0)v_c(q)+O(q^{-4}). \tag{3.25}$$

Equation (3.24) implies the presence in $V^{\rm pol}_{\uparrow\uparrow}(r)$ of a term $-2U_0(n_l)\,\delta(\mathbf{r})/n_l$, with $U_0(n_l)>0$, given by Eq. (3.17) with $d=3$. On the other hand, from Eq. (3.25) one obtains that for $r\to 0$, $V^{\rm pol}_{\uparrow\downarrow}(r)=2g(0)e^2/r$. This looks quite strange at first, as one would naively expect that at short distance effective interelectronic interactions should be essentially Coulombic. In fact, polarization potentials are not effective potentials, though at times this is not appreciated. We should also mention that in the approach of Refs. 35 and 36 the polarization potentials were assumed regular at the origin, $V^{\rm pol}_{\sigma\sigma'}(0)=e^2q_{\sigma\sigma'}$, with the screening wave vectors $q_{\sigma\sigma'}$ of the order of the Fermi wave vector q_F.

Effective electronic interactions were defined for the electrons gas by Kukkonen and Overhauser a long time ago,[37] using the polarization potential method but taking into ac-

count particle indistinguishability. According to this study effective two-body electron-electron interactions may be written as

$$V_{\sigma\sigma'}(q)=v_c(q)[1+\Delta_{\sigma\sigma'}(q)], \tag{3.26}$$

where

$$\Delta_{\sigma\sigma'}(q)=\frac{v_c(q)[1-G^s(q)]^2\chi_0(q)}{1-v_c(q)[1-G^s(q)]\chi_0(q)} \pm\frac{v_c(q)[G^a(q)]^2\chi_0(q)}{1+v_c(q)G^a(q)\chi_0(q)}, \tag{3.27}$$

with the upper (lower) sign corresponding to parallel (antiparallel) spins. The large-q behavior of $\Delta_{\sigma\sigma'}(q)$ is easily obtained from Eqs. (3.8), (3.22), and from the known asymptotic behavior[33] of the Lindhard function

$$\tilde{\chi}_0(q;n_l)_{q\to\infty}=-\frac{4mn_l}{\hbar^2q^2}. \tag{3.28}$$

One finds that $\Delta_{\uparrow\downarrow}(q)$ vanishes as q^{-2} for $q\to\infty$, while

$$\Delta_{\uparrow\uparrow}(q)_{q\to\infty}=-\frac{8}{27}r_s^3\left[\frac{d(r_s\tilde{\epsilon}_c)}{dr_s}\right]^2, \tag{3.29}$$

with $\tilde{\epsilon}_c(r_s)$ the correlation energy per particle, in Rydbergs, of the electron gas. Thus $V_{\uparrow\downarrow}(r)=e^2/r$ for small r, while the effective interaction between parallel spin is very slightly reduced with respect to the bare Coulomb repulsion, $V_{\uparrow\uparrow}(r)=\gamma(r_s)e^2/r$, with $\gamma(r_s)=1+\Delta_{\uparrow\uparrow}(\infty)\lesssim 1$. In particular, in the metallic regime one obtains from the known equation of state of the electron gas[38,39] $\gamma(r_s)=0.99$ and 0.98 for $r_s=2$ and 5. Thus, as we anticipated, effective interactions do remain essentially Coulombic at short distances.

IV. SECOND-ORDER THEORY

A. Three dimensions

We begin with the application of the second-order theory (SOT) to the freezing of superfluid ^{4}He. Experimental results on the system show that ^{4}He crystallizes[40] at a liquid density $n_l=0.0260$ Å^{-3} into an hcp-solid of density $n_s=0.0287$ Å^{-3}. We employ the Gaussian ansatz for a fcc-crystal density and apply Eq. (2.10) for the evaluation of the grand-potential difference between the solid and the liquid. The value of $\tilde{K}(q,n_l)$ at $q=0$ which enters in this calculation is related to the energy per particle $\epsilon(n_l)$ of the liquid via the ''compressibility sum rule,'' namely

$$-\tilde{K}(0;n_l)=2\epsilon'(n_l)+n_l\epsilon''(n_l), \tag{4.1}$$

where the primes denote differentiation with respect to the argument. For the quantity $\epsilon(n_l)$ we use an analytic fit based on accurate diffusion Monte Carlo data.[41]

We try to minimize $\Delta\Omega[n]$ [Eq. (2.10)] with respect to α for a variety of different values of (n_s,n_l). As can be seen in Fig. 5 for the pair of values which are close to those for which freezing occurs in experiments, $\Delta\Omega[n]$ has apparently *no minimum*; it keeps getting lower without bound as the localization increases. In the same figure it can be seen that for n_l much lower than the freezing value, $\Delta\Omega$ has a very

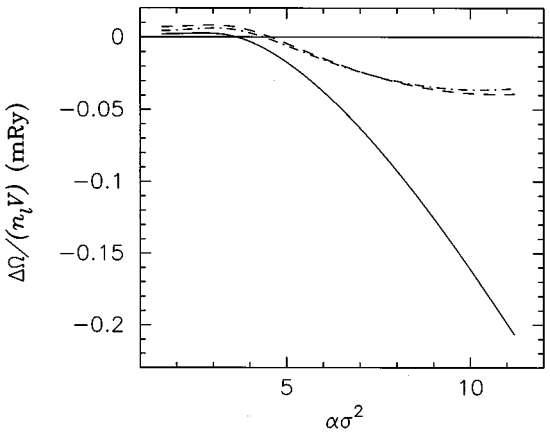

FIG. 5. Grand potential difference (Ref. 21) [Eq. (2.10)] between a ^{4}He fcc-solid and a liquid at the same chemical potential, for different pairs (n_s,n_l) in the second-order theory. Solid line: $n_s=0.0287$ Å^{-3}, $n_l=0.0262$ Å^{-3}; dashed line: $n_s=0.0287$ Å^{-3}, $n_l=0.0216$ Å^{-3}; dash-dotted line: $n_s=0.0275$ Å^{-3}, $n_l=0.019$ Å^{-3}. Here, $\sigma=2.556$ Å.

negative local minimum at strong localization (large values of α), i.e., the solid is predicted to be too stable. With reference to Fig. 5, note that at freezing one would expect $\alpha\sigma^2\approx 2$, in order to obtain the correct ''quantum'' Lindemann ratio $\gamma\simeq 0.3$. (γ is the ratio of the root-mean-square deviation about a site to the nearest-neighbor distance.) On the contrary, the minima shown in the figure are at $\alpha\sigma^2\approx 10$, implying a value of $\gamma\propto 1/\sqrt{\alpha}$ which is too small by about a factor 2, being essentially classical. Unfortunately, the lack of Monte Carlo data for the dcf at large wave vectors does not allow us to examine the limit of strong localizations, since as α grows we need more and more shells of RLV's into the sum of Eq. (2.10) in order to achieve convergence. Nevertheless, it is clear from the shape of $-\tilde{K}(q;n_l)$ (see Fig. 1) that the overestimation of the stability of the solid is brought about by the fact that $-\tilde{K}(q,n_l)$ is *negative* for all values of the RLV's; this way, the contribution from the excess part of the energy, which is becoming lower with increasing localization, dominates over the contribution from the ideal energy, which grows with localization, to yield a total energy which is *too low*. We will make this statement more quantitative shortly.

Next, we look at the SOT freezing of charged bosons, using the dcf-simulation results of Ref. 15. The system is known to undergo Wigner crystallization into a bcc-solid[38] at $r_s=160\pm 10$. Once more, we employ the Gaussian ansatz and try to minimize $\Delta E[n]$ [Eq. (2.15)] with respect to α at various different values of r_s. Some of the results are shown in Fig. 6. The quantity $\Delta E[n]$ is clearly unbounded from below, i.e. the absolute minimum lies at infinite localization, where the value of $\Delta E[n]$ is *minus infinity*. There is a local negative minimum at $\alpha r_0^2\approx 3$ for $r_s=50$. This corresponds to the correct quantum Lindemann ratio, and one might argue that the SOT of freezing may only make sense for modulations that are not too large (i.e., moderate values of α) and near the freezing density. Even so, the predicted freezing density would be overestimated by a factor of about 30.

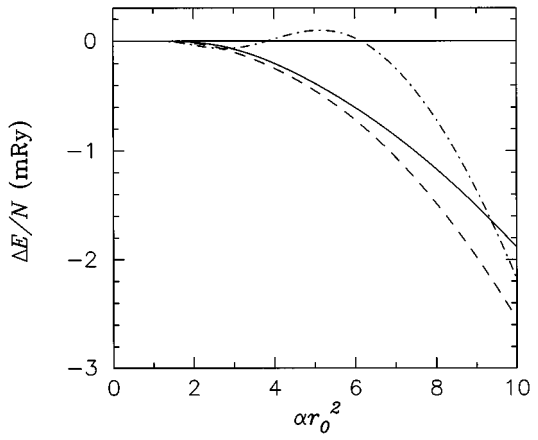

FIG. 6. Ground-state energy difference (Ref. 21) [Eq. (2.15)] between a charged boson bcc-solid and the liquid, versus localization at three different average densities, as obtained from the second-order theory. Solid line: $r_s=160$; dashed line: $r_s=100$; dash-dotted line: $r_s=50$.

It becomes clear, therefore, that the SOT suffers from the pathology of producing an unbounded functional. Within the framework of the Gaussian approximation, this feature can be clearly understood as follows. Take a solid whose lattice constant is a and consider the strong-localization limit, i.e., $\tilde{\alpha}\equiv\alpha a^2\gg 1$. In that case we have, with excellent accuracy, $\mu_2=0$ and $\mu_{\mathbf{Q}}=1$ for all $\mathbf{Q}$'s [see Eq. (2.26)]. In d dimensions, Eq. (2.23) gives

$$\left.\frac{T_0(\tilde{\alpha})}{Vn_l}\right|_{\tilde{\alpha}\gg 1}=(1+\eta)\frac{\hbar^2 d}{2ma^2}\tilde{\alpha}, \tag{4.2}$$

where $n_s=(1+\eta)n_l$ ($\eta=0$ for isochoric freezing). On the other hand, the excess energy contribution [i.e., the sum of the terms beyond T_0 on the rhs of Eq. (2.10) or Eq. (2.15)] may be conveniently broken into two contributions originating, respectively, from $\tilde{K}_R(q;n_l)$ and $\tilde{K}_S(q;n_l)$. The first contribution is most easily treated in reciprocal space, where it takes the form

$$\left.\frac{\Delta E^R_{\rm ex}(\tilde{\alpha})}{Vn_l}\right|_{\tilde{\alpha}\gg 1}=-\frac{\eta^2}{2}n_l\tilde{K}_R(0;n_l)-\frac{(1+\eta)^2}{2}\sum_{\mathbf{Q}\neq 0}e^{-(Qa)^2/4\tilde{\alpha}}n_l\tilde{K}_R(Q;n_l), \tag{4.3}$$

and manifestly tends to a constant for large values of α. The second contribution is evaluated in real space, to leading order, as

$$\left.\frac{\Delta E^S_{\rm ex}(\tilde{\alpha})}{Vn_l}\right|_{\tilde{\alpha}\gg 1}=-\frac{U_0(n_l)}{2Vn_l^2}\int d\mathbf{r}(\delta n(\mathbf{r}))^2=-\frac{U_0(n_l)(1+\eta)}{2n_l a^d\pi^{d/2}}\tilde{\alpha}^{d/2}, \tag{4.4}$$

using the fact that for $\tilde{\alpha}\gg 1$, the density reduces to a superposition of nonoverlapping normalized Gaussians $(2\alpha/\pi)^{d/2}\exp\{-2\alpha r^2\}$, one per site. The lack of a lower bound for $d=3$ can be now easily understood: since the ideal energy scales like $\tilde{\alpha}$ and the excess like $-\tilde{\alpha}^{3/2}$ for large $\tilde{\alpha}$, it is then clear that their sum will be dominated by the $-\tilde{\alpha}^{3/2}$ term and will be unbounded from below. The analysis presented above is valid also for fermions.

If a minimization within the restricted space of Gaussian profiles fails to yield a finite minimum, then the *global* minimum of the unrestricted Kohn-Sham (KS) scheme, which cannot be higher, will also be minus infinity. This does not exclude, however, the possibility of obtaining, by means of solving the KS equations, some *local* minimum at a moderate value of the localization; in the KS scheme there is no ''localization parameter'' of course, but the Lindemann ratio, for example, can be used as a measure of the spatial extent of the one-particle density around a lattice site. This possibility is particularly interesting because it could be argued that the perturbative character of the SOT immediately limits its validity to weakly modulated density profiles. In order to pursue this line, we have also performed the full, self-consistent calculation[7,9] for both charged bosons and spin-polarized electrons, within the SOT, at the densities for which the dcf is available (see Figs. 2 and 3 above). However, no local minimum was found, in either case. The large-q behavior of the dcf and the number of space dimensions render the SOT *pathological* in $d=3$.

B. Two dimensions

In two dimensions, Eqs. (4.2) and (4.4) show that both the ideal and excess term scale as $\tilde{\alpha}$ at strong localizations, the former with a positive and the latter with a negative coefficient. Therefore, the absolute values of the respective coefficients are crucial in determining the existence of a lower bound for the sum of the two terms. Expressing energies in Rydbergs and making use of Eqs. (4.2), (4.4), (3.17), and (3.13), we find for isochoric transitions ($\eta=0$):

$$\left.\frac{T_0(\tilde{\alpha};r_s)}{N}\right|_{\tilde{\alpha}\gg 1}=2\tilde{\alpha}\left(\frac{a_0}{a}\right)^2 \tag{4.5}$$

and

$$\left.\frac{\Delta E_{ex}(\tilde{\alpha};r_s)}{N}\right|_{\tilde{\alpha}\gg 1}=\frac{1}{2}r_s^2\frac{d(r_s\tilde{\epsilon}_c)}{dr_s}\tilde{\alpha}\left(\frac{a_0}{a}\right)^2, \tag{4.6}$$

where a is the lattice constant of the given crystal structure and $\tilde{\epsilon}_c$ the correlation energy per particle in Rydbergs. Thus, at strong localizations

$$\left.\frac{\Delta E(\tilde{\alpha};r_s)}{N}\right|_{\tilde{\alpha}\gg 1}\propto\left(2+\frac{1}{2}r_s^2\frac{d(r_s\tilde{\epsilon}_c)}{dr_s}\right)\tilde{\alpha}. \tag{4.7}$$

For polarized fermions ($\sigma=1$) in $2d$ the available QMC data[42,43] show that the coefficient in Eq. (4.7) is *positive* for $r_s\leqslant 59$. Therefore, the SOT functional remains bounded from below for values $r_s\leqslant 59$. This is encouraging, given that the polarized electron gas in two dimensions crystallizes into a triangular lattice at a value of r_s which is considerably smaller than this ''stability limit.''

We have thus performed a full Kohn-Sham calculation with the accurate liquid state input shown in Fig. 4, using a

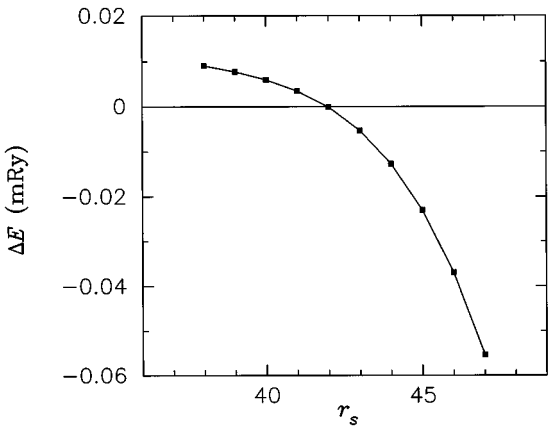

FIG. 7. Ground-state energy difference between triangular-solid and polarized liquid for electrons in $2d$ as function of the density. $\Delta E/N$ (in mRy) was calculated within the SOT. The solid squares are calculated points, with the line just a guide for the eye.

plane-wave basis set as explained at length elsewhere.[7,9] We have systematically checked convergence with respect to the plane-wave cutoff and the number of k points in the Brillouin zone. As it can be seen in Fig. 7 at $r_s=40$, where we have the dcf from QMC,[32] the solid is still unstable, though its energy is only 6 microRydbergs higher than that of the polarized liquid. On the ground that the explicit dependence of $G(q/q_F;r_s)$ on r_s should be very weak,[32] we have neglected it altogether to perform the calculations at the other values of r_s, using therefore the available local-field factor $G(q/q_F;r_s=40)$. This treatment predicts freezing from the polarized fluid at $r_s=42$ which agrees within error bars with the QMC prediction of Tanatar and Ceperley[42] $r_s=37\pm5$ and is within two error bars from a more recent QMC prediction[43] $r_s=34\pm4$. We have also evaluated the Lindemann ratio γ, which is shown in Fig. 8 as function of r_s near freezing. We find $\gamma=0.33$ at $r_s=42$, to be compared with an accepted value for quantum freezing of about 0.3. We may thus conclude that the SOT is capable of predicting freezing in two dimensions with good accuracy.

We have also investigated the effect of using a Gaussian ansatz for the Bloch orbitals (see, e.g., Sec. II C), as opposed

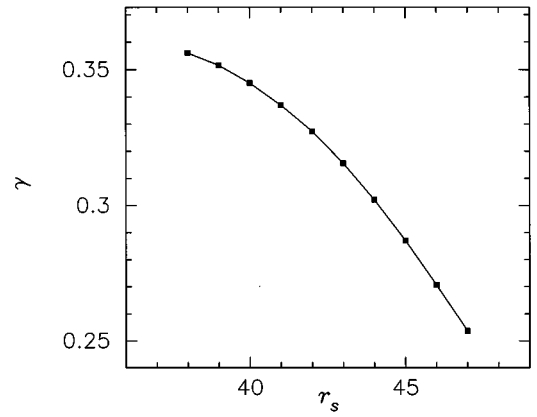

FIG. 8. Lindemann ratio γ around freezing in the triangular $2d$ Wigner crystal, as predicted by the SOT. The solid squares are calculated points, with the line just a guide for the eye.

to the full Kohn-Sham calculation presented above. As expected, this yields solid energies that are slightly higher, predicting freezing at a lower density, i.e., at $r_s=50$ with $\gamma=0.25$. Though this is well out of the range predicted by QMC (see above) it is still a substantial improvement with respect to an earlier prediction[23] of $r_s\gtrsim80$, using the Gaussian ansatz and an approximate local-field factor.

We should also mention results recently obtained using another DFT scheme,[44] in which a local-density approximation (LDA) to the total energy of the modulated phase is augmented by gradient corrections[45] (GCDFT). This approach yields crystallization at $r_s=31$, but with a density which appears to be very little modulated. In fact we have repeated such calculations, solving the equivalent one-orbital self-consistent Kohn-Sham equations in full. We reproduce the $r_s=31$ found in Ref. 44 and we find $\gamma=0.369$ which is very close to the uniform limit of $\gamma=0.373$. To give a more direct idea of what this means in terms of localization, we may look at the minimum in the density profile at half distance between a site and one of its nearest neighbors, in units of the on-site density, $\delta=n(r_{\rm NN}/2)/n(0)$. Here $r_{\rm NN}$ is the nearest-neighbor distance. We find that the GCDFT predicts $\delta=0.92$ at freezing, to compare with $\delta=0.30$, which we have obtained within the SOT, and an exact value which is likely to be even smaller. With respect to a conventional LDA (Refs. 6 and 9) in which the noninteracting kinetic energy is treated without approximation, the GCDFT is introducing an overestimate of the kinetic cost of a modulation. For the small modulations predicted by the GCDFT, this may easily be checked by comparing, for instance at the first RLV of the triangular crystal, the exact $2d$ noninteracting response function[46,30] with the one corresponding to the GCDFT, $\chi_0^{\rm GC}(q)=-(\sigma m/2\pi\hbar^2)/[1+q^2/2q_F^2]$. One might be tempted to argue that, for small modulations, the approach of Ref. 44 would be more consistent than a conventional LDA,[47] in that it treats all the components of the energy on the same footing. However, the quality of the resulting density profile, which is indeed very poor, pointing to a weakly first-order if not a second-order transition, contradicts such a conclusion.

Returning to the effects of the large-q behavior of the quantum dcf on freezing we may conclude that these are far less drastic in two dimensions than in three. Notice, however, that if one tried to apply the quadratic theory for systems with $r_s>59$, one would obtain, also in two dimensions, the erroneous answer that the stable phase is a crystal with infinite localization. This demonstrates that the quadratic theory gives a reasonable description of solids whose thermodynamic parameters are not far away from the freezing ones. Deep inside the region of thermodynamic stability of the solid, the SOT loses its validity, even in those cases where it succeeds in predicting freezing. Having concluded the discussion of the quadratic theory in two and three dimensions, we now proceed with the nonperturbative approach, i.e. the MWDA.

V. MODIFIED WEIGHTED DENSITY APPROXIMATION

In this section we will examine the behavior and performance of the MWDA for the case of systems of charged particles. The general analysis will show that regardless of

statistics, the MWDA yields a functional which is *bounded* from below, i.e., at the limit of large localizations the energy difference between the solid and the liquid tends to $+\infty$ and not $-\infty$ as in the case of the SOT. Then, we will present the application of the MWDA to the case of charged bosons, for which the availability of liquid-state input allows us to perform the MWDA calculation. We still find the stability of the crystal to be overestimated, nevertheless.

The presence of a singular term in the dcf $K(r;n_l)$ implies the existence of a similar term in the weight function $w(r;\hat{n})$, as is clear from Eqs. (2.18) and (3.16). With a straightforward analysis which closely parallels the one developed in the previous section for the excess energy one is led to the conclusion that for strong localizations (large values of the parameter α), the weighted density is given to leading order in α by

$$\hat{n}=\frac{U_0(\hat{n})}{-2\hat{n}\epsilon'(\hat{n})\pi^{d/2}}\alpha^{d/2}, \tag{5.1}$$

suggesting that $\hat{n}$ grows with α as we shall demonstrate shortly, provided that $-\hat{n}\epsilon'(\hat{n})>0$. We have verified that indeed $-\hat{n}\epsilon'(\hat{n})=(1/d)\hat{r_s}\epsilon'(\hat{r}_s)>0$ for all the systems considered below.[42,39,15] We shall examine the behavior of $\hat{n}$ in two and three space dimensions separately.

A. Charged fermions in two dimensions

On account of Eq. (5.1) above, let us assume that $\hat{n}$ diverges with α and therefore that $\hat{r}_s$—the Wigner radius in units of Bohr radii corresponding to the effective density $\hat{n}$—goes to zero in the same limit. Using the definitions of the previous section we may eliminate $\hat{n}$ in favor of $\hat{r}_s$ to obtain

$$\frac{1}{\hat{r}_s^2}=\frac{-(\hat{r}_s\epsilon_c(\hat{r}_s))'}{\hat{r}_s\epsilon'(\hat{r}_s)}\frac{C}{r_s^2}\widetilde{\alpha}, \tag{5.2}$$

with the prime denoting differentiation with respect to $\hat{r}_s$ and C a constant which depends on the structure chosen for the solid. Here ϵ_c and ϵ are, respectively, the correlation and the excess energy (exchange plus correlation) of the two-dimensional electron gas.

For small r_s the excess energy is given by[43]

$$\epsilon(\hat{r}_s)=-A\hat{r}_s^{-1}-B-D\hat{r}_s\ln\hat{r}_s+\ldots, \tag{5.3}$$

with A,B,D positive constants which depend on the spin polarization. The dominant, $-\hat{r}_s^{-1}$ term is the exchange energy and the remainder is the correlation energy $\epsilon_c(\hat{r}_s)$. Using the above equation and keeping only the leading terms in the ratio appearing in Eq. (5.2) one obtains at once

$$\hat{r}_s=(Ar_s^2/BC)^{1/3}\widetilde{\alpha}^{-1/3}. \tag{5.4}$$

Now, using Eq. (2.16) and since the excess energy of the liquid scales like $-\hat{r}_s^{-1}$ Eq. (5.4) yields

$$\left.\frac{E_{\rm ex}^{\rm MWDA}(r_s,\widetilde{\alpha})}{N}\right|_{\widetilde{\alpha}\gg 1}=-|E_{2d}(r_s)|\widetilde{\alpha}^{1/3}. \tag{5.5}$$

Since the ideal term scales as $\widetilde{\alpha}$, it dominates over the excess one at large $\widetilde{\alpha}$ and thus the total energy tends to plus infinity at the limit of strong localization. Notice that in the SOT the excess term scales as $-\widetilde{\alpha}$, whereas here only as $-\widetilde{\alpha}^{1/3}$. The MWDA makes the dependence of the excess energy on the localization parameter a lot weaker than the SOT. We will see that this is also the case in three dimensions.

B. Charged bosons and fermions in three dimensions

In three dimensions, eliminating $\hat{n}$ in favor of $\hat{r}_s$ in Eq. (5.1) yields

$$\frac{1}{\hat{r}_s^3}=\frac{-(\hat{r}_s\epsilon_c(\hat{r}_s))'}{\hat{r}_s\epsilon'(\hat{r}_s)}\frac{C}{r_s^3}\widetilde{\alpha}^{3/2}, \tag{5.6}$$

where ϵ_c and ϵ have the usual meaning for fermions, whereas for bosons ϵ_c coincides with ϵ—the total energy per particle. Again, C is a constant depending on the structure assumed for the solid. As in two dimensions, we are led to assume that $\hat{r}_s\to 0$ as $\widetilde{\alpha}\to\infty$ and therefore we shall retain in this limit only leading terms in Eq. (5.6).

Charged bosons. As we have already mentioned $\epsilon_c(\hat{r}_s)=\epsilon(\hat{r}_s)$ in this case and as $\hat{r}_s\to 0$, we have to dominant order $\epsilon(\hat{r}_s)=-0.8031\hat{r}_s^{-3/4}$ Ry.[15,48] Thus we obtain

$$\hat{r}_s=(3/C)^{1/3}r_s\widetilde{\alpha}^{-1/2}. \tag{5.7}$$

The energy $\epsilon(\hat{r}_s)$ now scales as $-\hat{r}_s^{-3/4}$ thus

$$\left.\frac{E_{\rm ex}^{\rm MWDA}(r_s,\widetilde{\alpha})}{N}\right|_{\widetilde{\alpha}\gg 1}=-|E_b(r_s)|\widetilde{\alpha}^{3/8}. \tag{5.8}$$

The MWDA-excess energy per particle scales only as $-\widetilde{\alpha}^{3/8}$ as opposed to $-\widetilde{\alpha}^{3/2}$ in the SOT. Thus, the ideal energy which is linear in $\widetilde{\alpha}$ dominates for strong localizations, and the MWDA functional is free of the pathology of the SOT, i.e., it does have a lower bound.

The actual calculations that we carried out were for the case of bosons only; however, the same analysis can be carried out for fermions, and the results for this case are presented below.

Charged fermions. The first few terms in the expansion of the excess ground-state energy of the electron fluid for small $\hat{r}_s$ read as[39]

$$\widetilde{\epsilon}(\hat{r}_s)=-B\hat{r}_s^{-1}+\Gamma\ln\hat{r}_s-\Delta+O(\hat{r}_s), \tag{5.9}$$

where all constants are positive. Once more, the term proportional to $-\hat{r}_s^{-1}$ is the exchange energy and the remainder is the correlation energy. Using Eqs. (5.6) and (5.9) we obtain as $\hat{r}_s\to 0$

$$\frac{1}{\hat{r}_s^3}=\hat{r}_s|\ln\hat{r}_s|\frac{\Gamma C}{B}\frac{1}{r_s^3}\widetilde{\alpha}^{3/2}. \tag{5.10}$$

To leading order as $\widetilde{\alpha}\to\infty$ we immediately obtain

$$\hat{r}_s = D(r_s)\frac{\tilde{\alpha}^{-3/8}}{[\ln\tilde{\alpha}]^{1/4}}, \tag{5.11}$$

with $D(r_s)=[8Br_s^3/3\Gamma C]^{1/4}$. Finally, since the excess energy per particle scales as $-\hat{r}_s^{-1}$ the MWDA functional obeys the scaling

$$\left.\frac{E_{\rm ex}^{\rm MWDA}(r_s,\tilde{\alpha})}{N}\right|_{\tilde{\alpha}\gg 1} = -|E_f(r_s)|[\ln\tilde{\alpha}]^{1/4}\tilde{\alpha}^{3/8}. \tag{5.12}$$

Thus, the MWDA is free of the unboundedness problem also for fermions. It is interesting that the scaling of the excess energy is now dependent on the statistics [see Eqs. (5.8) and (5.12) above], though very weakly, due to the logarithmic dependence in $\tilde{\alpha}$ present for fermions. This is at variance with the prediction of the SOT, where the same scaling was found and it appears intriguing. In fact, naive considerations would suggest that the excess energy should scale in the same way for bosons and fermions at the strong localization limit since, in this case, each particle is confined to its own cell and statistics becomes unimportant.

The existence of a lower bound for the MWDA functional is an improvement over the behavior of the SOT. However, this property guarantees neither the existence of a minimum at nonzero localization nor its correct location and behavior in terms of changes of the average density. If, for example, the total energy is monotonically increasing as a function of α, then the only minimum will occur for the uniform liquid. On the other hand, it is possible that a minimum always exists, for any value of the average density and is lower than the liquid one; in this second case, we are led to the erroneous prediction that the crystal is stable at all densities. In the following subsection we show the results of the full MWDA calculation for charged bosons and we find that, in fact, this second scenario materializes.

C. MWDA calculation for charged bosons

We have implemented the MWDA-self-consistency condition [Eq. (2.19)] for the case of charged bosons for which there exist sufficient simulation data for the local-field factor for a range of densities varying from $r_s=10$ to $r_s=160$ (Ref. 15). We have used an analytic fit to the equation of state obtained from simulation.[15] We limit our study to the charged boson liquid because for polarized fermions the only available Monte Carlo data are for $r_s=100$ and the implementation of the MWDA requires the knowledge of the dcf of the liquid over a wide range of densities.

We have carried out the MWDA calculation with the Gaussian ansatz for three different values for the average density, namely $r_s=20$, 50, and 100. The results are shown in Fig. 9. It can be seen immediately that, unlike the SOT, the MWDA gives minima of $\Delta E/N$ for finite values of the localization parameter α. Moreover, the trends of these minima are correct: they get deeper and also move towards stronger localization as the average density decreases. However, according to simulations[38] the liquid is stable for $r_s<160\pm 10$, whereas the MWDA gives a *lower* energy for the bcc solid for values of r_s as low as 20. Thus we can say that although the MWDA is already much better than the SOT, it still predicts a solid that is *too stable*. Even at high densities the MWDA functional has a global minimum for a modulated phase.

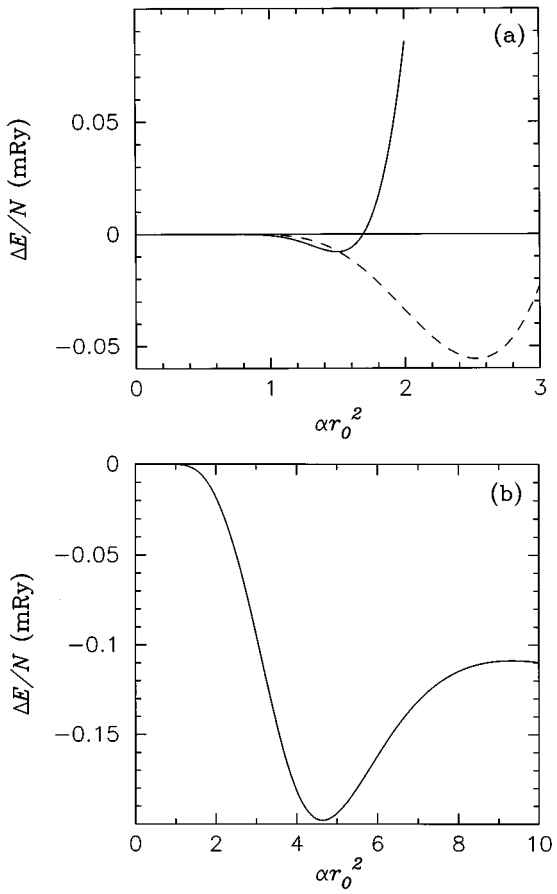

FIG. 9. Ground-state energy difference (Ref. 21) between the the charged boson bcc-solid and the liquid, versus localization at three different average densities, as obtained in the MWDA. (a) Solid line: $r_s=20$; dashed line: $r_s=50$. (b) $r_s=100$.

VI. CONCLUSIONS

The implementation of the correct liquid-state input in a density-functional approach to the freezing of quantum liquids brings about a remarkable new result, namely that *in three dimensions* the standard SOT suffers from a lack of a lower bound and is always *strictly* minimized for infinitely localized solids. As we have already mentioned, one might argue that the perturbative character of the SOT limits its validity to weakly modulated density profiles and thus local minima for finite localization should suffice. However, as we have demonstrated above for ^{4}He and charged bosons, such minima—when they exist—still yield an incorrect description of freezing, predicting stability of the solid well inside the region where the system in fact is liquid. Recourse to nonperturbative theories including certain classes of higher-order terms, such as the MDWA, does not help much in practice. One gets rid of the extreme pathology of the SOT theory in that the resulting functional is bounded from below, which is certainly satisfactory. However even the MDWA predicts the crystal to be the stable phase deep into the region where the liquid should be stable.

The asymptotic analysis in the localization parameter $\tilde{\alpha}$ that we have carried out above for the MDWA is easily generalized to the weighted density approximation (WDA),[49,9] once it is realized that the weight function $\tilde{w}(q;n)$ has in this case the same large-q limit as in the MWDA, and therefore the same singular term in real space. One obtains the same scalings as discussed in Sec. V above, and therefore bounded functionals. Whether the predictions of the WDA for freezing will be any better than those of the MWDA remains to be investigated, though we doubt it. The conventional LDA (Refs. 6 and 9) also brings about bounded functionals, as one may easily demonstrate, along similar lines as those illustrated above for the MWDA and WDA. The scaling is the same as for the MWDA for electrons in two dimensions and charged bosons in three dimensions; it is different for electrons in three dimensions, for which the exchange-correlation energy goes like $-\tilde{\alpha}^{1/2}$. Again, the LDA is making the solid too stable in three dimensions.[7]

The situation in two dimensions appears specular to the one summarized above for three dimensions. In fact, earlier applications of the DFT theory of freezing with approximate liquid dcf gave good results in three dimensions,[7,8] while failing in two dimensions.[23] We have demonstrated above that the reverse is true, if more accurate liquid input is used, which obeys the exact large-q behavior discussed in Sec. III. In particular, in two dimensions the SOT provides bounded functionals, in the relevant region of density, and yields a good description on the freezing transition.

The recently obtained accurate information on the liquid-state linear-response functions gives rise, therefore, to a new problem: our favorite approximate density-functional schemes which we have learned to trust from our experience on classical systems, seem to fail when applied to quantum systems in three dimensions. There is a need for reexamination of the current formalism of quantum density-functional theory of freezing and the development of approximate schemes which will be more appropriate to deal with the peculiarities of quantum systems. In this respect, the use of direct correlation functions possessing the correct asymptotic behavior is crucial, as is such a behavior that causes all the present troubles. At variance with the classical case we have seen that quantum functionals tend to predict excess energies (per particle) that negatively diverge at infinite localization. Though the MWDA produces a functional bounded from below, we speculate that the divergence of its excess part in this limit could still be incorrect, as the potential energy should remain finite, unless one can prove that it is the kinetic contribution to the excess energy which is bringing about this divergence.

ACKNOWLEDGMENTS

We would like to thank Professor S. Stringari both for helpful discussions and for sending us unpublished material and Dr. A. R. Denton for sending us a copy of Ref. 27 prior to publication. S.M. and G.S. also acknowledge fruitful collaboration with Dr. A. Debernardi in early work on the freezing of the $2d$ electron gas. C.N.L. has been supported by the Human Capital and Mobility Programme of the Commission of the European Communities, Contract No. ERBCHBICT940940.

*Present address: Institut für Festkörperforschung, Forschungszentrum Jülich GmbH, D-52425 Jülich, Germany.

†Electronic address: moroni@ictp.trieste.it

‡Electronic address: senatore@axpts0.ts.infn.it

[1] P. Hohenberg and W. Kohn, Phys. Rev. **136**, B864 (1964).

[2] N. D. Mermin, Phys. Rev. **137**, A1441 (1965).

[3] R. Evans, Adv. Phys. **28**, 143 (1979).

[4] Y. Singh, Phys. Rep. **207**, 351 (1991); for recent classical applications, see also, H. Löwen, *ibid.* **237**, 249 (1994).

[5] J. D. McCoy, S. W. Rick, and A. D. J. Haymet, J. Chem. Phys. **90**, 4622 (1989).

[6] W. Kohn and L. J. Sham, Phys. Rev. **140**, 1133 (1965).

[7] G. Senatore and G. Pastore, Phys. Rev. Lett. **64**, 303 (1990); in *High Pressure Equation of State: Theory and Applications*, CXIII Varenna School, Varenna, 1989, edited by X. S. Eliezer and R. A. Ricci (North-Holland, Amsterdam, 1991).

[8] A. R. Denton, P. Nielaba, K. J. Runge, and N. W. Ashcroft, Phys. Rev. Lett. **64**, 1529 (1990); J. Phys. Condens. Matter **3**, 593 (1991).

[9] S. Moroni and G. Senatore, Phys. Rev. B **44**, 9864 (1991).

[10] S. Moroni and G. Senatore, Europhys. Lett. **16**, 373 (1991).

[11] A. Holas, in *Strongly Coupled Plasma Physics*, edited by F. J. Rogers and H. E. Dewitt (Plenum, New York, 1987), p. 463.

[12] S. Stringari (private communication).

[13] S. Moroni, D. M. Ceperley, and G. Senatore, Phys. Rev. Lett. **69**, 1837 (1992).

[14] S. Moroni, D. M. Ceperley, and G. Senatore, Phys. Rev. Lett. **75**, 689 (1995).

[15] S. Moroni, S. Conti, and M. P. Tosi, Phys. Rev. B **53**, 9688 (1996).

[16] T. V. Ramakrishnan and M. Yussouff, Phys. Rev. B **19**, 2775 (1979).

[17] A. R. Denton and N. W. Ashcroft, Phys. Rev. A **39**, 4701 (1989).

[18] R. G. Parr and W. Yang, *Density Functional Theory of Atoms and Molecules* (Oxford University Press, New York, 1989).

[19] The functional inverse of a function $X(\mathbf{r},\mathbf{r}')$ is defined by $\int d\mathbf{r}'' X(\mathbf{r},\mathbf{r}'')X^{-1}(\mathbf{r}'',\mathbf{r}') = \int d\mathbf{r}'' X^{-1}(\mathbf{r},\mathbf{r}'')X(\mathbf{r}'',\mathbf{r}') = \delta(\mathbf{r}-\mathbf{r}')$, which in Fourier space and for an homogeneous system $[X(\mathbf{r},\mathbf{r}'')=X(|\mathbf{r}-\mathbf{r}''|)]$, as is the case here, yields $\tilde{X}^{-1}(q) = \int d\mathbf{r} e^{-i\mathbf{q}\cdot\mathbf{r}} X^{-1}(r) = 1/\tilde{X}(q)$, with $\tilde{X}(q) = \int d\mathbf{r} e^{-i\mathbf{q}\cdot\mathbf{r}} X(r)$.

[20] J. P. Hansen and I. R. MacDonald, *Theory of Simple Liquids*, 2nd ed. (Academic, New York, 1986).

[21] Note that, strictly speaking, these differences become differences of thermodynamic potentials *only* at the equilibrium density.

[22] K. S. Singwi and M. P. Tosi, *Solid State Physics: Advances in Research and Applications*, edited by H. Ehrenreich, F. Seitz, and D. Turnbull (Academic, New York, 1981), Vol. 36, p. 177.

[23] A. Debernardi, G. Pastore, and G. Senatore, in *Correlation in Electronic and Atomic Fields*, edited by P. Jena *et al.* (World Scientific, Singapore, 1989), p. 255.

[24] R. A. Aziz, V. P. S. Nain, J. S. Carley, W. L. Taylor, and G. T. Conville, J. Chem. Phys. **70**, 4330 (1979).

[25] M. H. Kalos, M. A. Lee, P. A. Whitlock, and G. V. Chester, Phys. Rev. B **24**, 115 (1981).

[26] F. Dalfovo, J. Dupont-Roc, N. Pavloff, S. Stringari, and J. Treiner, Europhys. Lett. **16**, 205 (1991).

[27] A. R. Denton, P. Nielaba, and N. W. Ashcroft (unpublished).
[28] In fact, phenomenological (Ref. 50) backflow corrections (Ref. 51) to the Feynman approximation, fitted to the observed response, yield a finite value of $n_l\widetilde{K}(\infty;n_l)$, in order-of-magnitude agreement with the very accurate values reported in the caption to Fig. 1.
[29] K. S. Singwi, M. P. Tosi, R. H. Land, and A. Sjölander, Phys. Rev. **176**, 589 (1968).
[30] S. Moroni, D. M. Ceperley, and G. Senatore, in *Strongly Coupled Plasma Physics*, edited by H. M. Van Horn and S. Ichimaru (Rochester University Press, Rochester, NY, 1993), p. 445.
[31] B. Farid, V. Heine, G. E. Engel, and I. J. Robertson, Phys. Rev. B **48**, 11 602, (1993).
[32] S. Moroni, D. M. Ceperley, and G. Senatore (unpublished).
[33] S. Yarlagadda and G. F. Giuliani, Phys. Rev. B **39**, 3386 (1989).
[34] G. Vignale, Phys. Rev. B **38**, 6445 (1988).
[35] See, e.g., D. Pines in *Highlights of Condensed-Matter Theory*, International School of Physics ''Enrico Fermi,'' Course LXXXIX, edited by F. Bassani *et al.* (North-Holland, Amsterdam, 1985), pp. 580–643.
[36] N. Iwamoto, E. Krotscheck, and D. Pines, Phys. Rev. B **29**, 3936 (1984).
[37] C. A. Kukkonen and A. W. Overhauser, Phys. Rev. B **20**, 550 (1979).
[38] D. M. Ceperley and B. J. Alder, Phys. Rev. Lett. **45**, 566 (1980).
[39] S. H. Vosko, L. Wilk, and M. Nusair, Can. J. Phys. **58**, 1200 (1980).
[40] E. R. Grilly, J. Low Temp. Phys. **11**, 33 (1973).
[41] S. Moroni, S. Fantoni, and G. Senatore, Phys. Rev. B **52**, 13 547 (1995).
[42] B. Tanatar and D. M. Ceperley, Phys. Rev. B **39**, 5005 (1989).
[43] F. Rapisarda and G. Senatore, Aust. J. Phys. **49**, 161 (1996).
[44] N. Choudhury and S. K. Ghosh, Phys. Rev. B **51**, 2588 (1995).
[45] See, e.g., N. H. March, in *Theory of the Inhomogeneous Electron Gas*, edited by S. Lundquist and N. H. March (Plenum, New York, 1983), pp. 1–77.
[46] F. Stern, Phys. Rev. Lett. **18**, 546 (1967).
[47] We have performed a conventional LDA calculation treating the noninteracting kinetic energy without approximations and we find freezing from the polarized $2d$ electron gas into the triangular lattice at an r_s as low as 15, with $\delta=0.40$.
[48] K. A. Brueckner, Phys. Rev. **156**, 204 (1967).
[49] W. Curtin and N. W. Ashcroft, Phys. Rev. A **32**, 2909 (1985).
[50] A. Kallio, M. Puoskari, and L. Lantto, in *Recent Progress in Many-Body Theories*, edited by H. Kummel and M.L. Ristig, Lecture Notes in Physics Vol. 198 (Springer, Berlin, 1984), pp. 198–218.
[51] R.P. Feynman and M. Cohen, Phys. Rev. **102**, 1189 (1956).